

Fig. 2 Calculated electrochemical windows (IP/EA) of different CCAs. All values are reported versus Mg/Mg<sup>2+</sup>. Red dots are EAs; blue dots are IPs.

and very low overpotential for Mg deposition.<sup>8c,d,9</sup> Further, Persson and Zavadil *et al.* found that the introduction of an electron-withdrawing substituent at the C-vertex of CCA improves the oxidation stability.<sup>10</sup> However, CCA Mg salts still suffer from low ion conductivity, due to their poor solubility in low viscosity solvents such as dimethoxyethane (DME) (Fig. 1B).<sup>8c,d,9,10</sup>

It has been experimentally established that halogenation of the B-vertices of CCA improves its weak coordinating ability and chemical stability by delocalizing and shielding the charge of the anion.<sup>11</sup> Therefore, this strategy has been traditionally utilized for the creation of super (Brønsted) acids<sup>12</sup> and highly activated cations (Fig. 1A).<sup>13</sup> However, modification of the B-vertices of CCA has not been investigated for MIB electrolytes, probably because halogenation of the B-vertices is expected to significantly decrease the reductive stability.<sup>14</sup> We wondered if this idea is correct. To address this question, we conducted theoretical and experimental studies on the effects of modification of the lower hemisphere (7–12-B vertices) of CCA on the solubility and conductivity.

## Results and discussion

To obtain insight into the redox stability of B-substituted CCAs, we commenced our study by computing the electrochemical window at the B3LYP-D3(BJ)/6-311++G(d,p) level, relative to the Mg/Mg<sup>2+</sup> redox pair set at 0.0 V (Fig. 2).<sup>15</sup> The electron affinity (EA) and ionization potential (IP) were calculated under the adiabatic approximation, which accounts for orbital and geometric relaxation between charge states. The EA is the energy gained for a reduced anion, while IP represents the energy penalty to oxidize an anion. The calculation of HCB<sub>11</sub>H<sub>5</sub>Br<sub>6</sub><sup>−</sup> (7–12-Br<sub>6</sub>-CCA), a commonly used WCA, indicated improved oxidative stability compared with CCA, to the same degree as FCB<sub>11</sub>H<sub>11</sub><sup>−</sup> (1-F-CCA), whereas the reduction stability was significantly decreased, which is consistent with the conventional idea.<sup>14</sup> Next, since electrophilic functionalization first

Table 1 Cyclic voltammetry of selected CCAs in HFIP<sup>a</sup> and MeCN<sup>b</sup>

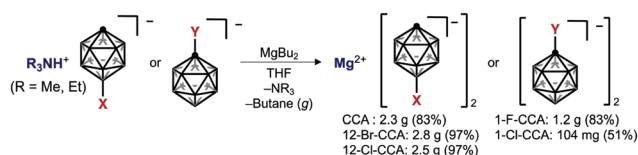
Compound	Oxidation (in HFIP) $E_{pa}^a$	Reduction (in MeCN) $E_{pc}^b$
[Bu <sub>4</sub> N] <sup>+</sup> [CCA]	2.08	— <sup>c</sup>
[Bu <sub>4</sub> N] <sup>+</sup> [7-12-Br <sub>6</sub> -CCA]	2.31	−2.85
[Bu <sub>4</sub> N] <sup>+</sup> [12-Br-CCA]	2.03	— <sup>c</sup>
[Bu <sub>4</sub> N] <sup>+</sup> [12-Cl-CCA]	2.07	— <sup>c</sup>

<sup>a</sup> The values are ordered by their cathodic peak potentials (CV value). All values [V] are referenced against the Fe<sup>0/+</sup> redox couple. Oxidations of TBA-CCAs were performed with [nBu<sub>4</sub>N]<sup>+</sup>[PF<sub>6</sub>]<sup>−</sup> as a supporting electrolyte. <sup>b</sup> Reduction measurements of TBA-CCAs were performed with [nBu<sub>4</sub>N]<sup>+</sup>[AsF<sub>6</sub>]<sup>−</sup> as a supporting electrolyte. <sup>c</sup> No reduction was observed within the available range of the solvent/electrolyte system.

occurs at the 12-B vertex, we computationally examined 12-*mono*-functionalized derivatives. Notably, DFT calculations showed that electronic perturbation at the 12-position of CCA has little or no effect on the cathodic stability. In contrast, the anodic stability depends markedly on the character of the substituent. The introduction of electron-withdrawing halogens at the 12-B vertex does not have a significant impact on the anodic stability, whereas electron-donating groups such as CH<sub>3</sub> at the 12-position decrease the anodic stability. Oxidized and reduced states of the 12-iodinated compound HCB<sub>11</sub>H<sub>10</sub>I<sup>−</sup> (12-I-CCA) were decomposed during geometry optimization, implying that the B–I bond is unstable in the redox process.<sup>16</sup>

To evaluate experimentally the effects of halogenations of the lower hemisphere, several CCAs other than 12-F-CCA, which requires extremely dangerous hydrogen fluoride for synthesis,<sup>17</sup> were then synthesized as the tetrabutylammonium (Bu<sub>4</sub>N) salts.<sup>18</sup> As expected from the DFT calculations, the 12-halogenated compounds HCB<sub>11</sub>H<sub>10</sub>Cl<sup>−</sup> (12-Cl-CCA) and HCB<sub>11</sub>H<sub>10</sub>Br<sup>−</sup> (12-Br-CCA) showed comparable oxidative stability to the parent CCA (Table 1). On the other hand, the oxidation stability of 7–12-Br<sub>6</sub>-CCA was significantly improved, but the reduction stability was significantly decreased.<sup>19</sup> However, 12-Cl-CCA and 12-Br-CCA showed no reduction in the same way as the parent CCA, suggesting that compounds halogenated at the 12-B vertex are potentially attractive as novel electrolytes without reducing redox stability.

The solubility of various *mono*-functionalized CCAs was next examined and compared that of unsubstituted CCA. Mg salts of *mono*-functionalized CCAs were prepared using Persson and Zavadil's elegant “deprotonative magnesiation” protocol (Scheme 1).<sup>10</sup> This method yields only butane (gas) and NR<sub>3</sub> (R = Me, Et) as by-products, and we found that it could be used to synthesize pure Mg salts on a gram scale. The “cation exchange”



Scheme 1 Synthesis of Mg salts of functionalized CCAs.



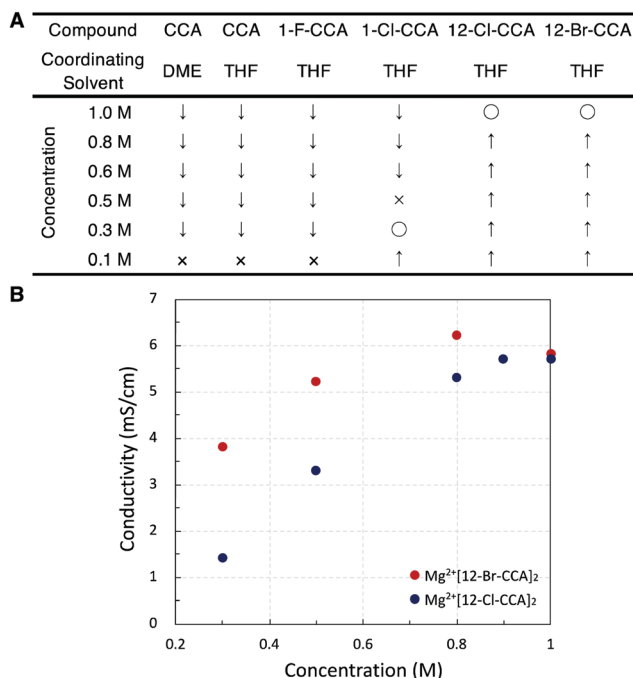


**Fig. 3** (A) Dissolution behavior of CCA derivatives in DME (○: soluble, ×: insoluble). (B) Ionic conductivity measurements of  $\text{Mg}^{2+}[\text{12-Cl-CCA}]_2$  in DME and  $\text{Mg}^{2+}[\text{12-Br-CCA}]_2$  in DME at various salt concentrations.

method<sup>8c</sup> starting from the Ag salts of CCAs proved to be unsuitable for large-scale synthesis of high-purity samples.

Since most Mg salts with WCAs coordinate with solvents such as DME or THF, we compared two kinds of unsubstituted compounds ( $\text{Mg}^{2+}[\text{CCA}]_2 \cdot \text{DME}$  and  $\text{Mg}^{2+}[\text{CCA}]_2 \cdot \text{THF}$ ) which differ in the coordinating solvent (DME or THF), in order to exclude the effect of coordinating solvents on the solubility of Mg salts (Fig. 3A).  $\text{Mg}^{2+}[\text{CCA}]_2 \cdot \text{DME}$  and  $\text{Mg}^{2+}[\text{CCA}]_2 \cdot \text{THF}$  showed the similar solubility in DME (<0.1 M), indicating that the type of coordinating solvent has little effect. Thus, for further investigations, we adopted Mg salts containing THF as the coordinating solvent. The 1(C-vertex)-fluorinated compound  $\text{Mg}^{2+}[\text{1-F-CCA}]_2$ , which was reported to show improved

oxidative stability,<sup>10</sup> was practically insoluble in DME (<0.1 M), and the 1-chlorinated compound  $\text{Mg}^{2+}[\text{1-Cl-CCA}]_2$  showed low solubility in DME (~0.3 M). In contrast, 12-B vertex halogenated compounds  $\text{Mg}^{2+}[\text{12-Cl-CCA}]_2$  and  $\text{Mg}^{2+}[\text{12-Br-CCA}]_2$  exhibited high solubility in DME (~1 M). Thus, the introduction of halogen at the 12-B vertex markedly improves the solubility. In terms of cation-negative charge interaction, the Coulombic attraction between a +1 point charge placed 2.5 Å from the hydrogen atom of a vertex on the B-H/C-H axis and the natural atomic charge in the anion increases in the order 1-C << 2-6-B < 7-11-B < 12-B positions, as shown by Michl *et al.*, for unperturbed CCA.<sup>20</sup> Therefore, substitution of the hydrogen atom with an electronegative, lower charge density, sterically shielding, and lipophilic halogen (Br or Cl) at the 12-B vertex should inhibit the interaction between CCA and the  $\text{Mg}^{2+}$  cation center more effectively than substitution at the 1-C vertex, and this is presumably the reason for the remarkably improved solubility of  $\text{Mg}^{2+}[\text{12-Cl-CCA}]_2$  and  $\text{Mg}^{2+}[\text{12-Br-CCA}]_2$ . Thus, based on the computational and fundamental physicochemical studies, we found that simple halogenation at 12-B vertex is an effective approach to increase solubility without decreasing redox stability.

The ionic conductivities of  $\text{Mg}^{2+}[\text{12-X-CCA}]_2$  (X = Cl and Br) at various concentrations in DME at room temperature were then measured (Fig. 3B). The ionic conductivities increased with increasing concentration, and reached maximum values at around 1.0 M for  $\text{Mg}^{2+}[\text{12-Cl-CCA}]_2$  in DME (5.6 mS/cm) and 0.8 M for  $\text{Mg}^{2+}[\text{12-Br-CCA}]_2$  in DME (6.2 mS/cm). These values are higher than those of conventional CCA-based  $\text{Mg}^{2+}$  salts, such as 0.65–0.85 M  $\text{Mg}^{2+}[\text{CCA}]_2$  in G3 (2.9 mS/cm) and 60 mM  $\text{Mg}^{2+}[\text{1-F-CCA}]_2$  in G3 (0.14 mS/cm).<sup>8c,10</sup> The reason for this is that the solubility in low viscosity solvent is drastically improved by the substitution at the 12-position.

Finally, we measured the electrochemical properties of  $\text{Mg}^{2+}[\text{12-X-CCA}]_2$  (X = Cl and Br) to examine the compatibility of these electrolyte solutions with Mg anodes. The cyclic voltammograms are shown in Fig. 4A. They exhibited excellent Mg deposition with very low overpotential ( $\leq 200$  mV) and high Coulombic efficiency (CE): CE of more than 95% was

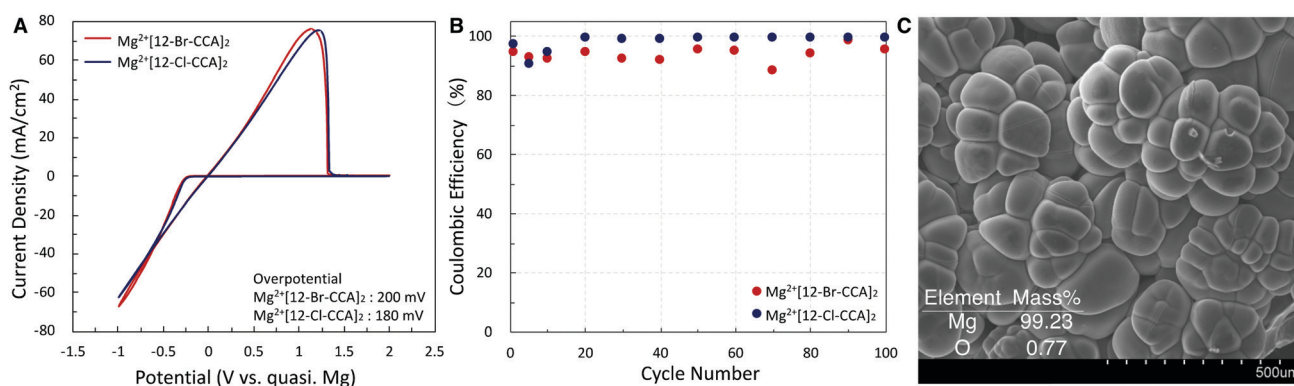


**Fig. 4** (A) Cyclic voltammograms of 1.0 M  $\text{Mg}^{2+}[\text{12-Cl-CCA}]_2$  and 0.8 M  $\text{Mg}^{2+}[\text{12-Br-CCA}]_2$  in DME using Pt as the working electrode and Mg as the reference at a scan rate of 100 mV/s. (B) Cycling behavior of Coulombic efficiency. (C) Scanning electron microscopy (SEM) image of Mg deposited on the Pt substrate from  $\text{Mg}^{2+}[\text{12-Br-CCA}]_2$  in DME.



maintained for at least 100 cycles (Fig. 4B). The reduced product of  $\text{Mg}^{2+}[\text{12-Br-CCA}]_2$  on a Pt disk working electrode was also analyzed by means of SEM, and energy dispersive X-ray spectroscopy (EDS) mapping indicated that the product is pure Mg metal (Fig. 4C). Furthermore, the absence of B, C, and Br supports the high redox and chemical stability of the 12-X-CCA skeleton. Overall, the results demonstrate good compatibility of these electrolyte solutions with Mg anodes.

## Conclusions

In summary, our combined computational and experimental studies demonstrate that functionalization of the lower hemisphere of the CCA skeleton with an appropriate choice of elements/functional groups can improve the electrochemical and physicochemical properties, such as conductivity and solubility. In particular, simple halogenation at the 12-B vertex of CCA dramatically improves the solubility in low viscosity solvents without compromising redox stability.  $\text{Mg}^{2+}[\text{12-Cl-CCA}]_2$  and  $\text{Mg}^{2+}[\text{12-Br-CCA}]_2$  showed excellent reversible magnesium deposition/stripping, with high Coulombic efficiency ( $\geq 95\%$ ).

Given that CCA is readily customizable, we anticipate that CCAs will be an excellent platform for the development of electrolytes for MIBs. Further studies to develop a higher performance CCA-based electrolyte by means of combined functionalizations of the C and B vertices are ongoing in our laboratory.

## Conflicts of interest

There are no conflicts to declare.

## Acknowledgements

This work was partly supported by JSPS KAKENHI (S) (No. 17H06173) (to M. U.), JST CREST (No. JPMJCR19R2) (to M. U.), Foundation NAGASE Science Technology Development, Sumitomo Foundation (to M. U.), JSPS KAKENHI (No. 19K23621 and 20K15950) (to J. K.), and JSPS KAKENHI (B) (No. 17H03017) (to K. M.). A generous allotment of computational resources (Projects G19012) from HOKUSAI GreatWave (RIKEN) is gratefully acknowledged. We are grateful to Prof. Dr Mutsumi Kimura for helpful discussion.

## Notes and references

- 1 A. Ponrouch, J. Bitenc, R. Dominko, N. Lindahl, P. Johansson and M. R. Palacin, *Energy Storage Mater.*, 2019, **20**, 253.
- 2 D. Aurbach, Z. Lu, A. Schechter, Y. Gofer, H. Gizbar, R. Turgeman, Y. Cohen, M. Moshkovich and E. Levi, *Nature*, 2000, **407**, 724.
- 3 Z. Ma, D. R. MacFarlane and M. Kar, *Batteries Supercaps*, 2019, **2**, 115.
- 4 M. Salama, I. Shterenberg, H. Gizbar, N. N. Eliaz, M. Kosa, K. Keinan-Adamsky, M. Afri, L. J. W. Shimon, H. E. Gottlieb, D. T. Major, Y. Gofer and D. Aurbach, *J. Phys. Chem. C*, 2016, **120**, 19586.
- 5 (a) L. F. Wan and D. Prendergast, *J. Am. Chem. Soc.*, 2014, **136**, 14456; (b) T. Kimura, K. Fujii, Y. Sato, M. Morita and N. Yoshimoto, *J. Phys. Chem. C*, 2015, **119**, 18911.
- 6 (a) Z. Lu, A. Schechter, M. Moshkovich and D. Aurbach, *J. Electroanal. Chem.*, 1999, **46**, 203; (b) R. Jay, A. W. Tomich, J. Zhang, Y. Zhao, A. D. Gorostiza, V. Lavallo and J. Guo, *Appl. Mater. Interfaces*, 2019, **11**, 11414.
- 7 E. N. Keyzer, H. F. J. Glass, Z. L. Liu, P. M. Bayley, S. E. Dutton, C. P. Grey and D. S. Wright, *J. Am. Chem. Soc.*, 2016, **138**, 8682.
- 8 (a) Y. Shao, T. Liu, G. Li, M. Gu, Z. Nie, M. Engelhard, J. Xiao, D. Lv, C. Wang, J. G. Zhang and J. Liu, *Sci. Rep.*, 2013, **3**, 3130; (b) T. J. Carter, R. Mohtadi, T. S. Arthur, F. Mizuno, R. Zhang, S. Shirai and J. W. Kampf, *Angew. Chem., Int. Ed.*, 2014, **53**, 3173; (c) O. Tutusaus, R. Mohtadi, T. S. Arthur, F. Mizuno, E. G. Nelson and Y. V. Sevryugina, *Angew. Chem., Int. Ed.*, 2015, **54**, 7900; (d) S. G. McArthur, L. X. Geng, J. C. Guo and V. Lavallo, *Inorg. Chem. Front.*, 2015, **2**, 1101; (e) J. T. Herb, C. A. Nist-Lund and C. B. Arnold, *ACS Energy Lett.*, 2016, **1**, 1227; (f) Z. Zhao-Karger, M. E. G. Bardaji, O. Fuhr and M. Fichtner, *J. Mater. Chem. A*, 2017, **5**, 10815; (g) E. N. Keyzer, J. Lee, Z. Liu, A. D. Bond, D. S. Wright and C. P. Grey, *J. Mater. Chem. A*, 2019, **7**, 2677; (h) K. C. Lau, T. J. Seguin, E. V. Carino, N. T. Hahn, J. G. Connell, B. J. Ingram, K. A. Persson, K. R. Zavadil and C. Liao, *J. Electrochem. Soc.*, 2019, **166**, A1510; (i) J. Luo, Y. Bi, L. Zhang, X. Zhang and T. L. Liu, *Angew. Chem., Int. Ed.*, 2019, **58**, 6967.
- 9 For reviews, see: (a) S. P. Fisher, A. W. Tomich, S. O. Lovera, J. F. Kleinsasser, J. Guo, M. J. Asay, H. M. Nelson and V. Lavallo, *Chem. Rev.*, 2019, **119**, 8262; (b) S. P. Fisher, A. Tomich, J. Guo and V. Lavallo, *Chem. Commun.*, 2019, **55**, 1684; (c) B. Ringstrand and P. Kaszynski, *Acc. Chem. Res.*, 2013, **46**, 214.
- 10 N. T. Hahn, T. J. Seguin, K. C. Lau, C. Liao, B. J. Ingram, K. A. Persson and K. R. Zavadil, *J. Am. Chem. Soc.*, 2018, **140**, 11076.
- 11 For recent reviews on CCAs, see: (a) C. Douvris and J. Michl, *Chem. Rev.*, 2013, **113**, PR179; (b) R. N. Grimes, *Carboranes*, Elsevier, Amsterdam, 3rd edn, 2016; (c) N. S. Hosmane, *Boron Science: New Technologies and Applications*, Taylor & Francis Books/CRC, Boca Raton, FL, 2011; (d) R. N. Grimes, *Dalton Trans.*, 2015, **44**, 5939; (e) J. Kanazawa, Y. Kitazawa and M. Uchiyama, *Chem. – Eur. J.*, 2019, **25**, 9123.
- 12 For reviews, see: (a) C. A. Reed, *Chem. Commun.*, 2005, 1669; (b) C. A. Reed, *Acc. Chem. Res.*, 2010, **43**, 121; (c) C. A. Reed, *Acc. Chem. Res.*, 2013, **46**, 2567; (d) C. Knapp, Weakly coordinating anions: Halogenated borates and dodecaborates, in *Comprehensive Inorganic Chemistry II*, Elsevier, Amsterdam, 2013, vol. 1, p. 651; (e) I. M. Riddlestone, A. Kraft, J. Schaefer and I. Krossing, *Angew. Chem., Int. Ed.*, 2018, **57**, 13982. For selected examples of super (Brønsted) acid, see: (f) M. Nava, I. V. Stoyanova,



- S. Cummings, E. S. Stoyanov and C. A. Reed, *Angew. Chem., Int. Ed.*, 2014, **53**, 1131.
- 13 (a) S. Moss, B. T. King, A. de Meijere, S. I. Kozhushkov, P. E. Eaton and J. Michl, *Org. Lett.*, 2001, **3**, 2375; (b) V. Volkis, C. Douvris and J. Michl, *J. Am. Chem. Soc.*, 2011, **133**, 7801; (c) Y. Kitazawa, R. Takita, K. Yoshida, A. Muranaka, S. Matsubara and M. Uchiyama, *J. Org. Chem.*, 2017, **82**, 1931; (d) C. Douvris and O. V. Ozerov, *Science*, 2008, **321**, 1188; (e) O. Allemann, S. Duttwyler, K. K. Baldrige and J. S. Siegel, *Science*, 2011, **332**, 574; (f) B. Shao, A. L. Bagdasarian, S. Popov and H. M. Nelson, *Science*, 2017, **355**, 1403; (g) S. Popov, B. Shao, A. L. Bagdasarian, T. R. Benton, L. Zou, Z. Yang, K. N. Houk and H. M. Nelson, *Science*, 2018, **361**, 381.
- 14 In ref. 10, the authors stated “Furthermore, selective derivatization of B sites on the  $\text{HCB}_{11}\text{H}_{11}^-$  cage has been demonstrated to significantly increase the oxidative stability of the anion, although at the cost of decreased reductive stability in every case.” For further evidence supporting this idea, see: (a) R. T. Boere, C. Bolli, M. Finze, A. Himmelspach, C. Knapp and T. L. Roemmele, *Chem. – Eur. J.*, 2013, **19**, 1784; (b) A. Wahab, C. Douvris, J. Klima, F. Sembera, J. Ugolotti, J. Kaleta, J. Ludvik and J. Michl, *Inorg. Chem.*, 2017, **56**, 269.
- 15 (a) J. A. Pople and L. A. Curtiss, *J. Phys. Chem.*, 1987, **91**, 155; (b) S. P. Ong and G. Ceder, *Electrochim. Acta*, 2010, **55**, 3804; (c) S. P. Ong, O. Andreussi, Y. Wu, N. Marzari and G. Ceder, *Chem. Mater.*, 2011, **23**, 2979; (d) X. H. Qu, A. Jain, N. N. Rajput, L. Cheng, Y. Zhang, S. P. Ong, M. Brafman, E. Maginn, L. A. Curtiss and K. A. Persson, *Comput. Mater. Sci.*, 2015, **103**, 56; (e) N. N. Rajput, X. Qu, N. Sa, A. K. Burrell and K. A. Persson, *J. Am. Chem. Soc.*, 2015, **137**, 3411.
- 16 In ref. 14a and 14b, 7–12 or 2–12 iodinated CCAs were found to have much lower oxidation and reduction stability than the corresponding brominated and chlorinated CCAs.
- 17 S. V. Ivanov, A. J. Lupinetti, S. M. Miller, O. P. Anderson, K. A. Solntsev and S. H. Strauss, *Inorg. Chem.*, 1995, **34**, 6419.
- 18 The anodic stability of  $\text{Mg}^{2+}$  salt of the CCA electrolytes was studied by linear sweep voltammetry using aluminum electrode. The oxidation current was observed at 3.5 V, which corresponds to glyme solvent decomposition. Therefore, to evaluate the oxidation stability of CCAs, we measured oxidation stability of CCAs in HFIP. For details, see ESI.†.
- 19 No obvious Mg deposition and stripping peaks were detected from  $\text{Mg}^{2+}[\text{7-12-Br}_6\text{-CCA}]_2$ , see ESI.†.
- 20 I. Zharov, T. Weng, A. Orendt, D. Barich, J. Penner-Hahn, D. Grant, Z. Havlas and J. Michl, *J. Am. Chem. Soc.*, 2004, **126**, 12033.

